4D bioprinting: the next-generation technology for biofabrication enabled by stimuli-responsive materials

2017 Biofabrication 9 012001

(http://iopscience.iop.org/1758-5090/9/1/012001)

Biofabrication

TOPICAL REVIEW

4D bioprinting: the next-generation technology for biofabrication enabled by stimuli-responsive materials

Yi-Chen Li[1,2,3,7], Yu Shrike Zhang[1,2,3,7], Ali Akpek[1,2,4], Su Ryon Shin[1,2,3,8] and Ali Khademhosseini[1,2,3,5,6,8]

[1] Biomaterials Innovation Research Center, Division of Engineering in Medicine, Department of Medicine, Brigham and Women's Hospital, Harvard Medical School, Cambridge, MA 02139, USA
[2] Harvard-MIT Division of Health Sciences and Technology, Massachusetts Institute of Technology, Cambridge, MA 02139, USA
[3] Wyss Institute for Biologically Inspired Engineering, Harvard University, Boston, MA 02115, USA
[4] Department of Biomedical Engineering, Istanbul Yeni Yuzyil University, Istanbul 34010, Turkey
[5] Department of Physics, King Abdulaziz University, Jeddah 21569, Saudi Arabia
[6] College of Animal Bioscience and Technology, Department of Bioindustrial Technologies, Konkuk University, Hwayang-dong, Kwangjin-gu, Seoul 143-701, Korea
[7] Y C Li and Y S Zhang contributed equally to this work.
[8] S R Shin and A Khademhosseini contributed equally as corresponding authors to this work.

E-mail: sshin4@partners.org **and** alik@bwh.harvard.edu

RECEIVED
4 July 2016

REVISED
12 September 2016

ACCEPTED FOR PUBLICATION
7 October 2016

PUBLISHED
1 December 2016

Keywords: 4D bioprinting, 3D bioprinting, shape-changing, smart biomaterials

Abstract

Four-dimensional (4D) bioprinting, encompassing a wide range of disciplines including bioengineering, materials science, chemistry, and computer sciences, is emerging as the next-generation biofabrication technology. By utilizing stimuli-responsive materials and advanced three-dimensional (3D) bioprinting strategies, 4D bioprinting aims to create dynamic 3D patterned biological structures that can transform their shapes or behavior under various stimuli. In this review, we highlight the potential use of various stimuli-responsive materials for 4D printing and their extension into biofabrication. We first discuss the state of the art and limitations associated with current 3D printing modalities and their transition into the inclusion of the additional time dimension. We then suggest the potential use of different stimuli-responsive biomaterials as the bioink that may achieve 4D bioprinting where transformation of fabricated biological constructs can be realized. We finally conclude with future perspectives.

1. Introduction

Engineered artificial tissues that biologically and physiologically resemble their counterparts *in vivo* can be used to repair damaged or diseased tissues [1–4]. Alternatively, *in vitro* tissue models have also recently attracted increasing attention with an aim of improving current platforms to more accurately predict responses of pharmaceutical compounds in the human body, thus expediting the drug development process [5–10]. To this end, three-dimensional (3D) bioprinting has emerged as a versatile technique to create biomimetic tissue constructs at unprecedented spatial precision and freedom [11–13].

In 1986, the first 3D printing technology was reported by Hull and co-workers [14]. They described a process termed stereolithography (SLA), where 3D constructs could be fabricated via layer-by-layer crosslinking of the resin through synchronized UV exposure and upward movement of the stage. This layer-by-layer technique enabled direct generation of complex objects at very high precision not achievable with the traditional manufacturing and machining procedures. A series of other 3D printing methods have also been developed over the years such as fused deposition modeling [15], selective laser melting [16], and selective laser sintering techniques [17–19]. While the conventional 3D printing strategies such as inkjet, microextrusion, and laser-assisted printers were used for generation of non-cellular structures, more recently these techniques have been further developed to enable 3D fabrication of biological structures directly encapsulating cells and bioactive agents, including various biomimetic tissues such as the blood vessels, liver, heart, and tumors [20–22].

Most native tissues exhibit complex 3D shapes, structures, microarchitectures, and extracellular matrix compositions, as well as possessing unique functions that are achieved through dynamic changes in tissue conformations. For example, the heart has a four-chambered configuration, which along with rhythmic contraction governed by the intrinsic electrical system, exhibits a strong and regular pumping behavior to achieve blood circulation through the body [23]. In addition, similar electrical signals transmitted from the brain can induce the movement of the musculoskeletal system, such as the peristaltic moves of esophagus or gut that consist of sequential, alternating waves of contraction and relaxation of alimentary wall smooth muscles, which act to propel food along [24–26]. The movements can also be directed by other biochemical cues such as nitric oxide that leads to vasodilation and caffeine that causes vasoconstriction. Most these dynamic conformational changes of tissues that render them functional are caused by built-in mechanisms that respond to intrinsic and/or external stimuli, adding a fourth dimension to the biological system.

Therefore, the conventional 3D structures featuring static properties and behaviors obtained from 3D bioprinting may not suffice the need for use in biomedicine. The recently developed four-dimensional (4D) bioprinting technology based on 3D bioprinting but with the embedded ability of shape transformation may solve this challenge and more accurately mimic the dynamics of the native tissues. In this strategy, stimuli-responsive biomaterials are integrated with the 3D bioprinting technology to fabricate biologically active constructs that can alter their shapes upon desired stimulation to achieve prescribed functionality.

In this review, we highlight recent advances in the development of 4D bioprinting techniques and their potential applications in biomedicines. We discuss the state of the art 3D printing and bioprinting modalities along with their associated challenges. In addition, the potential use of different stimuli-responsive biomaterials, including thermal-, humidity-, electrical-, magnetic-, and photo-sensitive materials as programmable bioinks, is discussed for their capability to achieve 4D bioprinting. We finally propose future directions and perspectives to further develop novel 4D bioprinting platforms in mimicking architectures and function of native biological tissues.

2. Current 3D bioprinting techniques and their limitations

2.1. 3D printing and bioprinting modalities

A variety of techniques have been developed for 3D printing [21, 27–29]. Fused deposition modeling is the most common modality due to its low cost and simplicity [30]. In fused deposition modeling, the melted material is extruded out through a nozzle in a layer-by-layer manner until a desired 3D model is created. Materials suitable for fused deposition modeling include thermoplastics such as poly(lactic acid) (PLA). However, fused deposition modeling generally possesses relatively low resolution and long operation times. Laminated object manufacturing is another technique used for 3D printing. During a typical procedure, a belt of target material is cut out by the laser in the desired shape and repeated in a layer-by-layer manner, where all the layers are adhered together by the assistance of heating [31]. Laminated object manufacturing is a fast fabrication methodology but the substantial amount of waste material during the printing process has increased its cost. In selective laser melting, the printing material in the powder form fills the reservoir, which is subsequently exposed to a high-energy laser that melts the powders into desired shapes [32]. Repeated melting and solidification cycles will eventually lead to the fabrication of 3D constructs. Similar to selective laser melting, selective laser sintering also shapes models by laser [33], while the most common materials that are employed in selective laser sintering are metals and ceramics [34]. Similar to selective laser melting, the granulated material filling the reservoir is exposed by laser. Unlike selective laser melting, the major difference of selective laser sintering lies in that the granules of the material are sintered instead of melting, leaving larger grains and the porosity of the fabricated objects [35]. Additionally, SLA has also been widely used as a versatile 3D printing technology [27]. It is an additive manufacturing method, during the process of which a photosensitive pre-polymer is crosslinked layer-by-layer using patterned light, synergized with upward pulling of the printed object from the reservoir [28]. Recently this bioprinting technology has been adapted for applications in biofabrication. For example, Shaochen and colleagues developed a digital light processing-based stereolithographic process to create multi-component constructs with human induced pluripotent stem cells-derived hepatocyte-like cells in a biomimetic liver lobule pattern [36]. SLA printing enables high exquisiteness and resolution in the range of 0.05–0.15 mm.

Although these methodologies allow for convenient 3D printing of thermoplastics, metals, and ceramics, they are not necessarily compatible with biomaterials embedded with cellular components. During the past decade tremendous progress has been made in the development of 3D bioprinting, where both cells and bioactive molecules especially those in the form of hydrogels are integrated with 3D printers [11–13, 37–39]. Three common techniques of 3D bioprinting including inkjet, microextrusion, and laser-assisted printing, are illustrated in figure 1 [11]. The inkjet printing relies on ejection of a liquid bioink in the droplet form forced to build in the 3D volume on a substrate, through either piezoeletric [40] or thermal

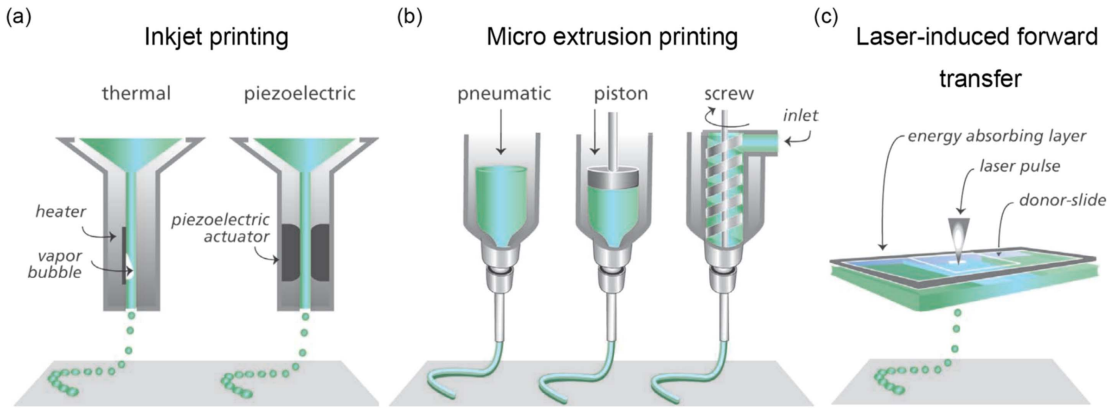

Figure 1. Three most common 3D bioprinting techniques: (a) inkjet bioprinters, (b) microextrusion bioprinters and (c) laser-assisted bioprinter. (Reprinted with permission from [12] Copyright (2013) Wiley.)

[41] actuation (figure 1(a)). This type of drop-on-demand bioprinter typically presents high printing speed at low cost. Another common modality for 3D bioprinting is microextrusion where the bioinks are physically extruded by a mechanical [42] or pneumatic [43] dispensing system (figure 1(b)). The major advantages of microextrusion printers include the continuity of the extruded bioinks rather than the discontinuous liquid droplet for the inkjet printers, the wide viscosity range of the bioinks that can be used, and high cell densities that may be achieved. Another widely used modality for bioprinting is termed laser-induced forward transfer [44–46]. This system consists of a laser-energy absorbing layer and bioink layer. When the focused laser pulses on the absorbing layer such as gold or titanium, a droplet containing the bioink and encapsulated cells is forced to deposit towards the collecting substrate to form the desired pattern (figure 1(c)). Since laser-induced forward transfer does not need a nozzle, the clogging problem with nozzle-based bioprinters can be avoided [47–49].

2.2. Challenges associated with 3D bioprinting

Due to the versatility of the technique, 3D printing has been extensively used in many areas such as those in electrical, mechanical, and biomedical engineering. However, there are several challenges associated with 3D printing especially when it comes to biomedicine. For example, the choice over the materials (i.e. the bioinks) has to be accurate to ensure robust transformation into 3D structures while maintaining sufficient viability and functionality of the embedded cells coherently [13]. On one hand, bioprinted structures may exhibit inhomogeneous cell densities in case the bioinks have overly low viscosities [50] and on the other hand, high-viscosity bioinks may cause increased shear stresses during the extrusion process that may affect cell viability and functions [51]. To this end, a microfluidic technique has been recently proposed for convenient deposition of low-viscosity bioinks, where a carrier sheath flow was used to assist the extrusion of the bioink delivered through the core of the printhead [52]. Moreover, a new technique termed embedded bioprinting further allowed direct anti-gravity writing of 3D freeform structures in a supporting matrix, which could be selectively removed to retrieve the bioprinted volumetric objects [53–55].

The inability of most current 3D bioprinting platforms to fabricate biological structures with high compositional complexity creates another major obstacle, since most systems can only achieve bioprinting of a single bioink during each deposition process. Thus, efforts have been presented during the last decade for the development of multi-material bioprinting modalities [52, 56–59]. For example, the Sun, Lewis, and Atala Groups separately developed multi-nozzle bioprinters capable of sequentially extruding several types of bioinks as well as polymeric scaffolding materials for the generation of complex tissue architectures [56, 59, 60]. Alternatively, a single microfluidic printhead design devised by the Khademhosseini and Lewis Groups enabled continuous and/or simultaneous deposition of two types of bioinks for production of heterogeneous or gradient structures [52, 58, 61].

While these two challenges require further technological developments in materials and instrumentation, the third obstacle described below might be readily overcome by rational integration of existing technologies. The conventional 3D bioprinted microenvironment may not be able to elicit proper biological responses since the structures cannot actively transform once printed, in contrast to the highly dynamic and constantly changing morphologies of native tissues against surrounding stimulants [62, 63]. Therefore, it is crucial to develop new methodologies for bioprinting objects that can undergo prescribed transformation as needed, by elegantly combining current 3D bioprinting platforms with a rich variety of already known stimuli-responsive biomaterials, thus leading to the emergence of 4D bioprinting.

3. Transition to 4D printing and bioprinting

Shape transformation is regarded as the fourth dimension added onto printed 3D structures. Mechanisms as complex as those in facilitating protein folding and origami that employ directed transformation are exciting and expected to evolve into 4D bioprinting in the years to come [64–69]. One of the simplest mechanisms that can be adopted for 4D printing and bioprinting however, lies in the deposition of heterogeneous materials that possess differential properties (e.g. swelling) to achieve folding and unfolding under proper conditions. Indeed, two pioneering examples using such strategy have opened new avenues for improved designs of engineered tissues, biomedical devices, and soft robotics, among others.

Tibbits and colleagues envisioned a combination of insights on both design and engineering aspect, and indicated that material programmability, multi-material printing techniques, and meticulous designs for accurate transformations are vital requirements for 4D printing [70]. In an early demonstration on 4D printing by the team, the transformation of the printed grid structures was reported. Materials capable of expanding to different degrees were used as the joints between two adjacent rigid segments, where the folding direction and angle of the joints could be controlled by regulating the material properties and tuning the position of the angle limiters (figure 2(a)). Consequently, under suitable stimulus the printed grid could transform into the desired sinusoidal wave or hyperbolic surface (figures 2(b) and (c)). More sophisticated transformation could be designed using this approach, such as the gradual conversion of the shape resembling 'MIT' into a pre-defined form 'SAL' (figure 2(d)).

Recently, a 4D biomimetic printing technique based on hydrogel materials was further reported by Lewis and co-workers [71]. They developed a printable ink consisting of synthetic hectorite clay, nanofibrillated cellulose, and the N, N-dimethylacrylamide or N-isopropylacrylamide (NIPAM) monomers, for fabrication of shape-morphing natural analogues such as the flowers, bracts, and leaves that could transform under stimulus. The technology relied on the anisotropic swelling properties controlled by aligning the orientations of cellulose fibrils within the hydrogel. During the process of printing, the extruded fibers possessed anisotropic swelling behaviors along the longitudinal direction since the cellulose component underwent a shear-induced alignment [72] as the ink was squeezed through the nozzle [73]. They harnessed the anisotropic swelling property of this bioink to precisely control their relative orientations and locations in bilayer structures to achieve different folding upon swelling (figure 2(e)). Figure 2(f) clearly demonstrates the folding of printed bilayer patterns into 3D flower-like structures using this biomimetic 4D printing technique. In particular, when the petals were printed in a bilayer structure with a 90°/0° angle arrangement, the resulting structure could mimic the closure of the flower (figure 2(f) (i)); on the contrary, if the fibers in the petals were printed at a 45°/45° configuration, a convoluted folding path was obtained (figure 2(f) (ii)). Combination of these folding mechanisms further enabled multiple shape-transformation events for the generation of a structure mimicking the orchid *Dendrobium helix*, by discrete dispositions of each petal when swollen in water (figures 2((f) (iii))–((f) (vi))).

Besides swelling, Studart and colleagues proposed another interesting idea of 4D printing based on magnetic materials. They developed an ink consisting of poly(urethane acrylate) (PUA) doped with modified aluminum platelets that could respond to an externally applied low magnetic field [74]. The aluminum platelets (shown in brown color) dispersed in the printed architecture underwent directed pattern transformation upon the application of a magnetic field during the printing and subsequent curing processes (figure 2(g)). Microscopic images further confirmed that the local orientations and alignments of the platelets well matched the patterns as programmed (figure 2(g) (iii) (vi)).

These few pioneering examples clearly demonstrated the possibility to incorporate the additional time scale into 3D printing to achieve transformation of fabricated objects along prescribed paths. However, these pioneering 4D printing techniques still require overcoming major challenges in mimicking the complex dynamic deformation of the native tissues such as the pumping behavior of the heart and the peristalsis moves of the esophagus/gut, among others. Combining bioactive agents and specific cell types with the 4D printing strategies provides a potential method to solve these challenges. To this end, it is necessary to develop a library of biocompatible stimuli-responsive materials that possess good cytocompatibility, provide mechanical support, and enable proper biophysical/biochemical signaling for the cells to induce programmed deformation under physiological stimuli, therefore achieving 4D bioprinting. In the next section we will introduce several categories of stimuli-responsive biomaterials that can be potentially used for 4D bioprinting to generate biomimetic tissue constructs with extended applications in biomedicine.

4. Stimuli-responsive mechanisms for 4D bioprinting

As the field of 4D bioprinting is just starting to emerge, we expect its rapid expansion in the years to come. The significantly enhanced usability and functionality of the bioprinted objects due to their capability to transform with time will likely find widespread applications in areas including but not limited to tissue engineering, regenerative medicine, bioelectronics, robotics,

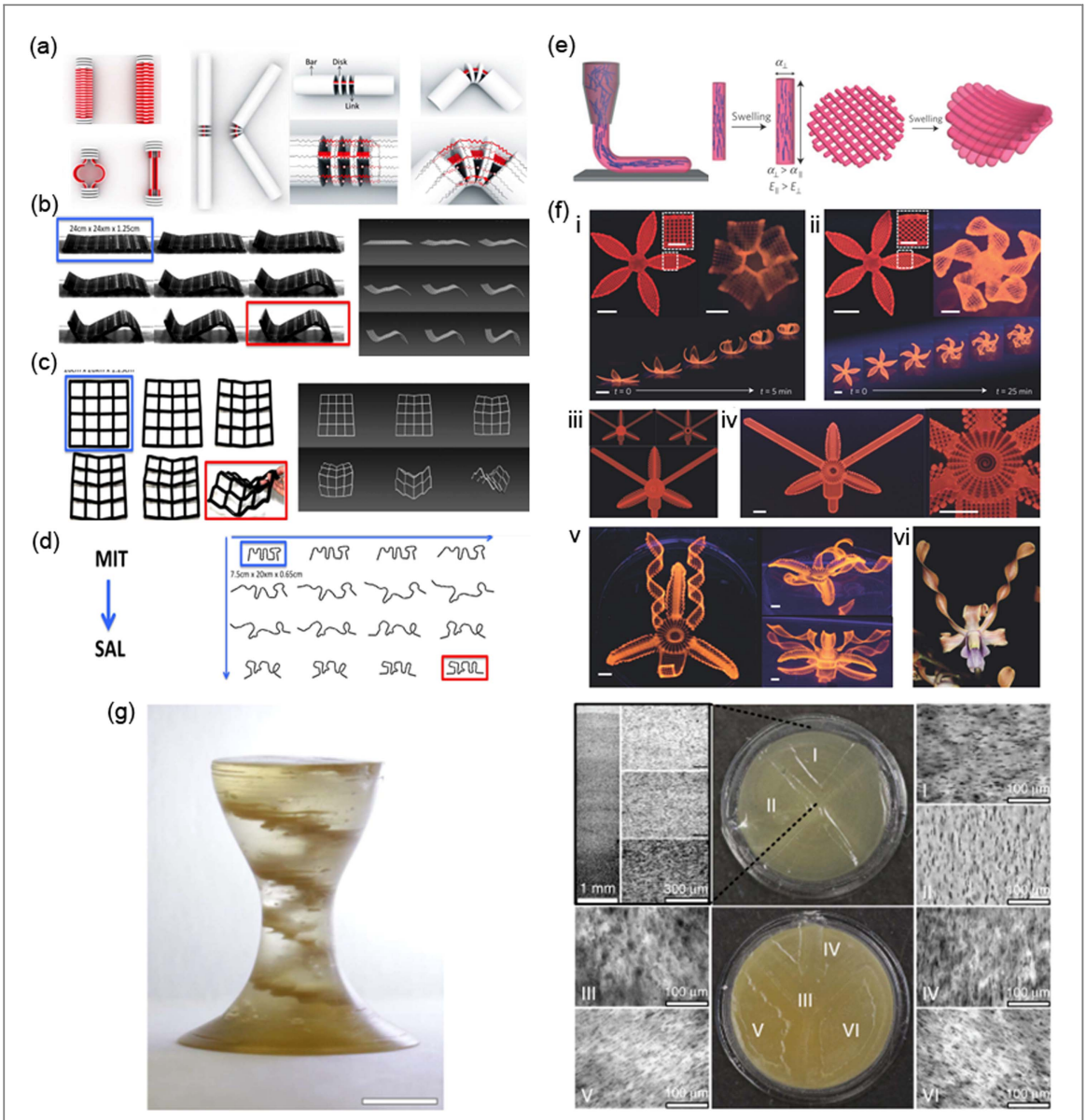

Figure 2. (a) The transformation of 4D printed objects. The transformation of the printed grid into (b) a sinusoidal wave and (c) a hyperbolic surface. (d) A time-varying curve showed the change of shape from MIT to SAL. (Reprinted with permission from [70] Copyright (2014) Nature Publishing Group.) (e) The schematic of programming the anisotropy of ink. (f) The morphologies of flower fabricated by biomimetic 4D printing. (i) 90°/0° bilayer. (ii) −45°/45° bilayer. The (iii) print bah, (iv) printed structure, and (v) swollen structure of a flower inspired by (vi) *Dendrobium helix*. (Reprinted with permission from [71] Copyright (2016) Nature Publishing Group.) (g) Internal helicoidally staircase was fabricated by 3D printed object containing magnetic nanoplates. (g) (i), (ii) Optical micrographs of the top layer of the structure show the local different alignment of aluminum platelets match the programmed architecture. (g) (iii), (vi) Optical micrographs of the bottom layer of the structure, showing the in-plane oriented platelets (III) and out-of-plane oriented platelets aligning with programmed directions (IV–VI). (Reprinted with permission from [74] Copyright (2015) Nature Publishing Group).

actuators, and even medical devices. Since there is limited number of demonstrations currently available in this new field, here we will review a series of transformation mechanisms based on either cells or stimuli-responsive biomaterials and discuss their potential integration with the 4D bioprinting technology.

4.1. Cell traction force (CTF) for 4D bioprinting

In addition to using material properties to provide transformation ability to the structures, another possibility lies in the utilization of cells as the active folding element to move 3D microstructures into pre-defined shapes. Cell origami is a technique that harnesses living cells as the driving force to implement the transformation of cell-laden patterns [75, 76]. CTF is considered as the major mechanism of cell origami due to the contractile force exerted by the cells originating from actin polymerization and actomyosin interactions [75]. CTF plays a critical role in many biological processes to regulate the cellular behaviors such as wound healing [77], angiogenesis [78], metastasis [79], and inflammation [80]. Also, CTF regulates several fold-forming processes of tissues during the development of an organism. For instance, the tension plays an

important role in gastrulation and neurulation during the body's development [81, 82].

Recently, Takeuchi and colleagues have applied basic principles of cellular origami to fabricate a 3D microstructure induced by CTF [83]. They developed a model where cells were seeded across two microplates attached onto a piece of glass substrate (figure 3(a)). Upon detaching from the glass directional folding of these microplates could be initiated (figure 3(b)). Subsequently, 3D cell-laden microstructures were fabricated using an assembly of multiple two-dimensional (2D) microplates (figure 3(c)). It was further possible to create various 3D cell-laden microstructures by properly designing the geometrical patterns of the assembled 2D microplates. In particular, with fibroblasts the group was able to successfully generate various hollow microstructures such as a cube, a dodecahedron, and a cylindrical helical tube, without using flexible joints or supporting materials (figures 3(d) and (f)). As indicated in figure 3(f), the cylindrical tube was fabricated by rolling up microplates along the diagonal lines, whose diameters could be controlled by modifying the angles of these lines. Using such a method, vessel-like structures were also fabricated by culturing vascular cells including human umbilical vein endothelial cells and human arterial endothelial cells. In addition, it was also demonstrated that this cell-enabled folding technique had the capability to produce 3D microstructures such as the dodecahedron in a high-throughput manner (figure 3(g)). Confocal images confirmed that hollow structures were present within these cell-laden dodecahedrons (figure 3(g)). These features have indicated the feasibility to fold 2D microplates into 3D cell-laden microstructures by taking advantages of CTF. Cell origami is a simple technique that potentially enables 4D bioprinting, and when multiple cell types are combined complex cell-laden structures mimicking their native counterparts may be spontaneously formed in a post-printing procedure.

4.2. Smart biomaterials for 4D bioprinting

4.2.1. Humidity-responsive materials

Humidity-responsiveness is widely present in nature. For example, when the humidity is low the flake of pinecone will spontaneously open to assist the seed dispersion and the wheat awns will twist due to the heterogeneity present in these structures [84–86]. As the humidity shifts in the surrounding environment, some of the biological systems release or absorb moistures. These phenomena thus inspired the development of humidity-responsive materials [87, 88]. Naumov and co-workers developed a new material whose motion could be quickly actuated upon humidity change [89]. They combined the poly(ethylene glycol) (PEG)-conjugated azobenzene derivative (PCAD) and agarose (AG) (PCAD@AG) to fabricate a composite substrate. AG is a natural material capable of rapid absorption of water but low desorption. On the contrary, PCAD was used to decrease the rate of absorption and enhance desorption to establish a humidity-responsive system. This design was critical for the rapid locomotion of PCAD@AG film, which deflected upon exposure to the environmental humidity (figure 4(a)).

Thiele and co-workers further formulated a humidity-responsive cellulose-based material [90]. They fabricated a bilayer film consisting of a cellulose stearoyl ester with a low substitution degree of 0.3 ($CSE_{0.3}$) and a high substitution degree of 3 (CSE_3). When $CSE_{0.3}$ was exposed to humidity on one side, its surface absorbed water molecules and generated horizontal and vertical swelling forces (F_s) (figure 4(b)). On the contrary, CSE_3 was hydrophobic and had temperature-responsive properties. Therefore, the bilayer film possessed both hydrophilic and hydrophobic surfaces each exposed to one side. As shown in figure 4(b), the $CSE_{0.3}/CSE_3$ bilayer film was initially maintained at 55 °C and 5.9% relative humidity to achieve steady states of both layers and stabilize the film in a flat configuration. Subsequently, as the temperature was cooled down to 22 °C with relative humidity increased to 35% the bilayer film started to bend from the CSE_3 side, which slightly contracted; the $CSE_{0.3}$ layer followed to roll up due to swelling to eventually form a tight roll of the film. This process could be readily reverted when the bilayer film was again exposed to its original environment at 55 °C and 5.9% relative humidity. Additionally, the authors indicated that making the $CSE_{0.3}$ film with a gradient thickness could result in a non-symmetric bending movement for the cellulose-based materials. These examples recall the earliest versions of 4D printing technology and the concept of a multi-layer structure can be easily adapted to many future designs of 4D bioprinting, in conjunction with biocompatible humidity-responsive materials. However, the cell culture environment with a constantly high humidity (i.e. within the medium) will limit the transformation ability of each material to only a single time. In addition, the cells require a specific osmotic pressure. Therefore, the extent of shape-changing for humidity-responsive materials may be limited due to the limitation in the humidity/osmotic pressure that can be applied to the constructs. These challenges might be resolved by tuning the sensitivity of the humidity-responsive materials that can readily transform within the range of cell endurance.

4.2.2. Temperature-responsive materials

Thermo-responsive materials can employ the exogenous temperature changes as stimuli to achieve shape transformation [91]. In particular, the transformation principle of thermo-responsive hydrogels is based on their wettability and solubility alteration following the change of temperature [92, 93]. Temperature responsiveness is probably one of the most commonly

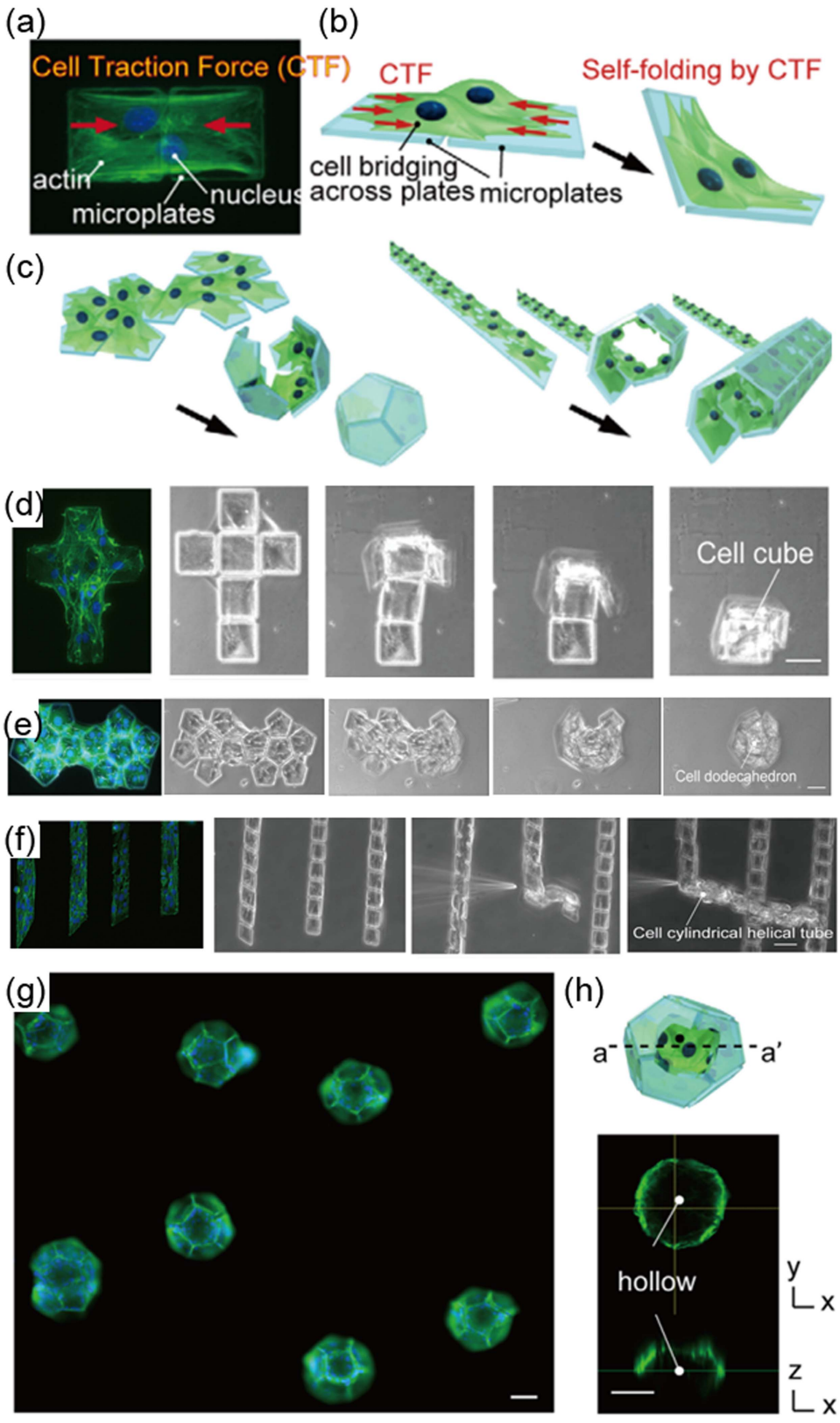

Figure 3. The 3D cell-laden structure formed by cellular origami. (a) Cells adhered on the two microplates. (b) The illustration of microplate was folded by CTF. (c) Three different types of 3D structures were formed by CTF. (d)–(f) Three transformed geometric structures: regular tetragon, regular dodecahedron, and cylindrical tube. (g) Fluorescent image of multiple dodecahedrons. (h) Confocal cross-sectional images of the hollow dodecahedron structure. Green: actin, blue: nucleus. Scale bars = 50 μm. (Reprinted with permission from [83] Copyright (2012) Public Library of Science.)

investigated mechanisms to achieve user-defined functionality [94, 95]. Hu and colleagues provided a basic idea to fabricate a double-network hydrogel that combined two components with drastically different thermal properties induced by crystallization of one component [93, 96–98]. Based on this concept, a

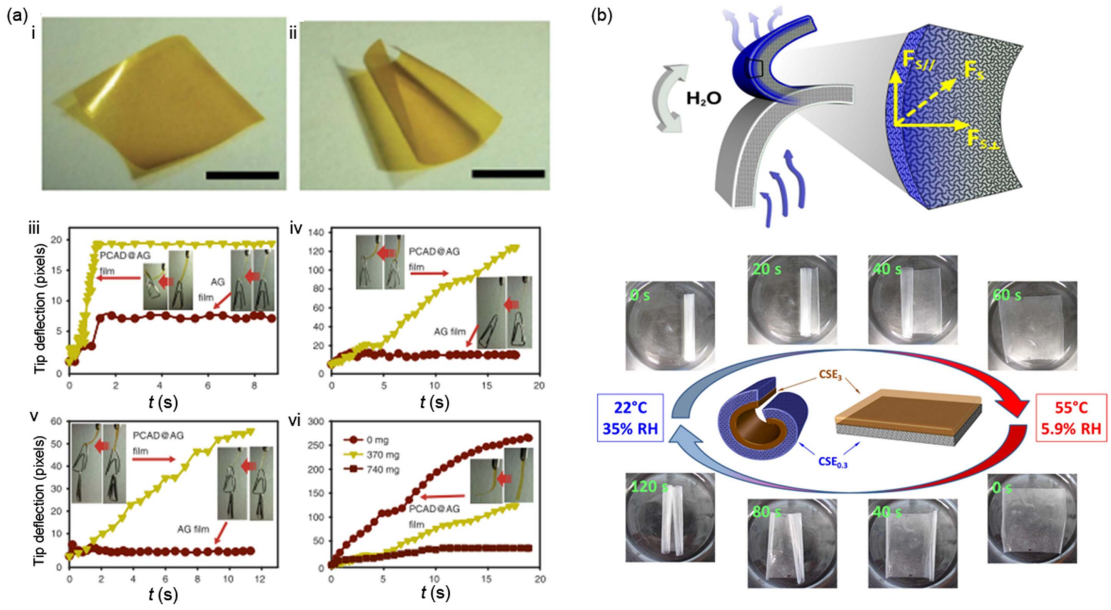

Figure 4. (a) The shape change of PCAD@AG film before (a) (i) and after (a) (ii) exposure of humidity. Humidity-induced bending of PCAD@AG film and pure AG with sizes of (a) (iii) 2 cm × 0.5 cm × 100 μm and (a) (iv) 2 cm × 0.5 cm × 200 μm loaded with a cargo of 370 mg. (a) (v) The doped versus undoped PCAD@AG film in humidity-induced bending. (a) (vi) Effect of cargo weight on PCAD@AG film. (Reprinted with permission from [89] Copyright (2015) Nature Publishing Group.) (b) The illustration and shape change of the humidity-responsive CES film is triggered by the absorption and desorption of water. (Reprinted with permission from [90] Copyright (2015) Nature Publishing Group.)

hydrogel was fabricated with poly(vinyl alcohol) (PVA) capable of crystallization interpenetrated with a chemically crosslinked PEG (figure 5(a)) [98]. When the hydrogel containing 70% PVA and 30% PEG (PEG-30) went through three cycles of freezing/thawing (PEG-30-3), the morphology of the hydrogel could be stabilized as a helix. The hydrogel was able to transform back to a straight line after 15 s of immersion in hot water (90 °C), at which temperature the crystalline domain of PVA melted. Additionally, deformed angle and x-ray diffraction analyses indicated that the crystallinity would increase when the freezing/thawing cycle was increased [99]; therefore PEG-30 with only one freezing/thawing cycle (PEG-30-1) showed fastest response compared to other samples that underwent more cycles. These results revealed that the degree of thermo-responsiveness could be regulated by the crystallinity of the polymers forming the hydrogel.

Xu and co-workers combined dynamic ionic bonds and covalent bonds to develop a new thermal-responsive thiol-ene-functionalized polybutadiene (PB) rubber [100]. As shown in figure 5(b), the ionic bonds were formed by the functionalized PB-COOH and PB-NH_2 and then crosslinked by different concentrations of trithiol crosslinker (i.e. synthesized PB (SPB)-0%, SPB-2%, and SPB-6%). The SPB-6% hydrogel was processed into a permanent spiral-like structure by photocrosslinking the SPB film rolled on a rod. When the spiral hydrogel was heated to 60 °C, the structure transformed into a temporary flat shape, which could be further fixed upon cooling. Interestingly, it was observed that the spiral-like structure spontaneously recovered after being reheated to 60 °C. The mechanism of transformation might be caused by the thermo-reversibility of the ionic bonds. During the heating process, the broken ionic bonds resulted in the transformation of the film, which were then reconstructed after cooling to lock the shape; during the reheating stage, the bonds became broken again and the stored strain was released, and consequently the recovery stress drove the film to return to its original spiral structure.

Poly(N-isopropylacrylamide) (pNIPAM) is known as one of the most used thermo-responsive materials [101]. In pNIPAM hydrogel the polymer chains become hydrophilic when the environmental temperature is decreased to lower than the low critical solution temperature [102]. Breger and colleagues photocrosslinked acrylic acid-functionalized pNIPAM (pNIPAM-AAc) to polypropylene fumarate (PPF) [103]. As the temperature was raised to above 36 °C, the pNIPAM-AAc component transformed to a hydrophobic state to expose the PPF segments and thus achieve shape transformation (figure 5(c)). At the same time water was also expelled as the temperature was elevated resulting in increased ratio of dry weight-to-swollen weight of the hydrogel.

Moreover, Chen and colleagues utilized 4-hydroxybutyl acrylate (4HBA) as a crosslinker to generate a pNIPAM-OH hydrogel with a gradient porous morphology (figure 5(d)) [104]. By increasing the temperature to 40 °C, the sliced hydrogel disk folded upwards to assume a tubular shape within 35 s,

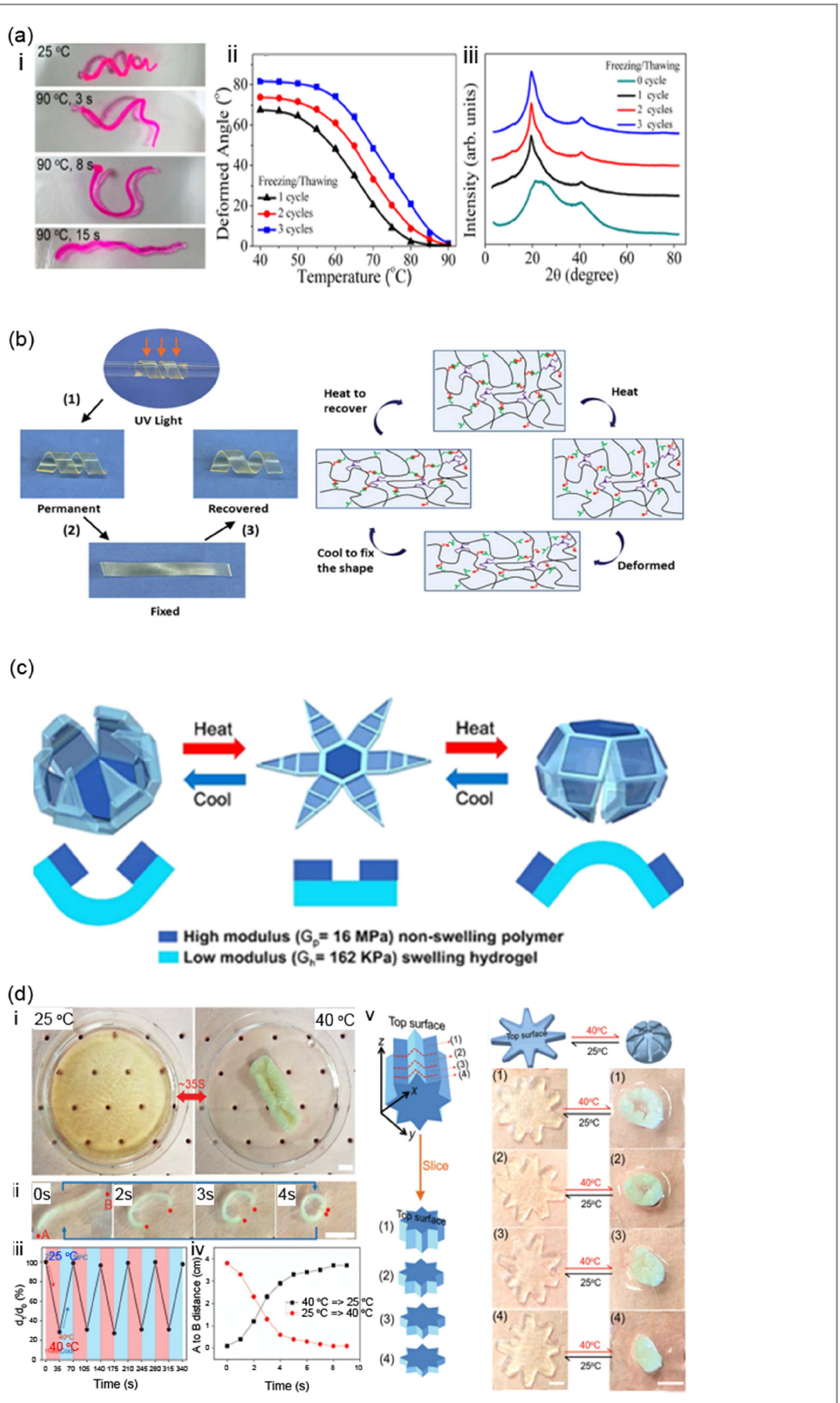

Figure 5. (a) (i) Photographs of thermal transformation of PEG30-3. (a) (ii) Plots of deformed angle versus temperature and (a) (iii) x-ray diffraction patterns of PEG-30 hydrogel underwent different freezing/thawing cycle. (Reprinted with permission from [98] Copyright (2015) American Chemical Society.) (b) The image and mechanism of shape memory behaviors of SPB-6% at a cooling (20 °C) and heat/reheat (60 °C) temperature. (Reprinted with permission from [100] Copyright (2015) Royal Society of Chemistry.) (c) Schematics of the transformion behaviors of the thermal-responsive microgripper. (Reprinted with permission from [103] Copyright (2015) American Chemical Society.) (d) (i) The morphology change of a gradient porous hydrogel at 20 °C and 40 °C. (d) (ii) The thermal responsive time of the hydrogel strip was placed at 40 °C water. (d) (iii) The reversible size change and responsive time of the hydrogel after thermal stimulation. (d) (iv) The end-to-end distance of the hydrogel strip after the alternative heating/cooling stimulation. (d) (v) The folding behaviors of sliced hydrogels with random thickness after thermal stimulation. (Reprinted with permission from [104] Copyright (2015) John Wiley & Sons).

through anisotropic motion caused by the gradient in pore sizes. The hydrogel also presented a strong reversibility, where no significant differences after 10 cycles of shape changes were observed. Also, Spinks and coworkers used a thermal-responsive alginate/pNIPAM ink to print a smart valve to control the flow of water by the hydrogel valve at 20 °C (swollen, closed state) and 60 °C (shrunken, open state) [105].

These different types of thermo-responsive materials have been widely used in various applications including tissue engineering, drug delivery, and sensing, and are thoroughly characterized for their properties including for example, biocompatibility. Therefore, they potentially offer a great value for 4D bioprinting where shape transformation can be achieved by temperature alteration within a reasonable range. However, these pNIPAM-based thermal-responsive materials lack bioactivity and generally require relatively high transformation temperatures leading to insufficient cell viability and functions. This challenge might be solved by using copolymers with pNIPAM to reduce the transformation temperature to around 37 °C to maintain high cell viability, and by combining bioactive peptides (e.g. arginine–glycineaspartic acid (RGD)) and molecules (e.g. growth factors) to improve the cell adhesion and growth.

4.2.3. Electrical and magnetic-responsive materials

Most electrical-responsive smart materials usually rely on their electrically conductive characteristic. The properties of such materials can be regulated by the intensity or the direction of the externally applied electrical field [106]. This feature provides new applications for biomimetic or bioinspired systems since the materials can change their size and/or shape in response to the electric stimulation [107, 108]. For example, dimensional changes in some electrically conductive materials such as polyaniline [109] and polypyrrole (PPy) [110] have been confirmed due to the electrochemical doping that transports ions between the materials and the surrounding electrolyte under applied electrical potential, thus facilitating shape transformation using these materials. Saido and colleagues presented a method where PPy film was doped with tetrafluoroborate, and then connected by a copper wire and a silver paste on the two ends, respectively (figure 6(a)) [111, 112]. Figure 6(b) shows a folded accordion-like construct, which was compressed and annealed to fix its shape. Upon stimulation by the electric potential, the PPy constructs expanded rapidly due to the desorption of water vapor by Joule heating, and achieved a maximum strain of 147% [103]. The elongation of the construct under electrical stimulation could be further controlled by the balance of the forces. A biomorphic robot was accordingly created by connecting two accordion-like constructs in series. Plastic plates were assigned as pawls for this biomorphic robot. When a voltage of 3 V was applied for 5 s, the front pawl was pushed to move forward through expansion of the first accordion while the rear hook was fixed by the ratchet teeth on the substrate to prevent it from sliding backwards; when the electric field was turned off for 10 s, the contraction force pulled the rear hook forward.

Carbon nanotubes (CNTs) are a class of biocompatible one-dimensional materials possessing excellent conductivity [113, 114]. Du and colleagues coated a sheet of CNTs with a shape-memory polymer Veriflex® [115]. Figure 6(c) shows the recovery of the shape-memory composite blended with 1.8 g CNT nanopaper under the application of an electric current of 0.09 A. It was observed that the flat shape-memory specimen was bended to a 'U'-like temporary shape, but restored to its original shape within 120 s upon release of the current. Therefore, it was confirmed that the electrical conductivity and the speed of electroactive response of the shape-memory composite could be significantly improved by CNTs. This information indicated that electrical-responsive materials might improve the electrical property of other materials and be useful for the applications in shape transformation or memory.

Besides, magnetic field is broadly used in the biomedical applications [116, 117]. For example, magnetic-responsive ferrogels have been used to control the release of a number of drugs [118, 119]. Mooney and colleagues recently developed an alginate-based scaffold with magnetic-sensitive capability and 3D interconnected macropores for drug and cell delivery [120]. To increase the adhesive and release abilities, they conjugated a cell-binding domain, RGD with alginate and iron oxide particles were embedded within the RGD-modified alginate. Under the magnetic field, strong and rapid compression could be activated for this macroporous ferrogel to drive the outward movement of water from the internal pores, triggering the release of cells or biological agent. As shown in figure 6(d), comparing the alginate-based ferrogels with the two pore sizes, the nanoporous ferrogels reduced only 5% in height at 38 A m^{-2}, while the macroporous ferrogels was compressed nearly 70% when subjected to the same magnetic field. Furthermore, the release of the cells from these ferrogels could also be controlled by the adhesion properties of the alginate matrix. Upon stimulation of a cyclic magnetic field, more cells could be released from the scaffold when the RGD modification degree was reduced for alginate in the ferrogels.

Furthermore, composite biocompatible inks based on a mixture of CNTs or magnetic particles with hydrogels have been recently developed for bioprinting of both 2D patterns and 3D structures [114, 120]. The bioprinted constructs were able to support the adhesion and growth of cells while showing high electrical conductivity. It is expected that, these bioinks when programmed to deposit into desired structures combined with proper electrical or magnetic stimuli will make 4D bioprinting possible. Although the

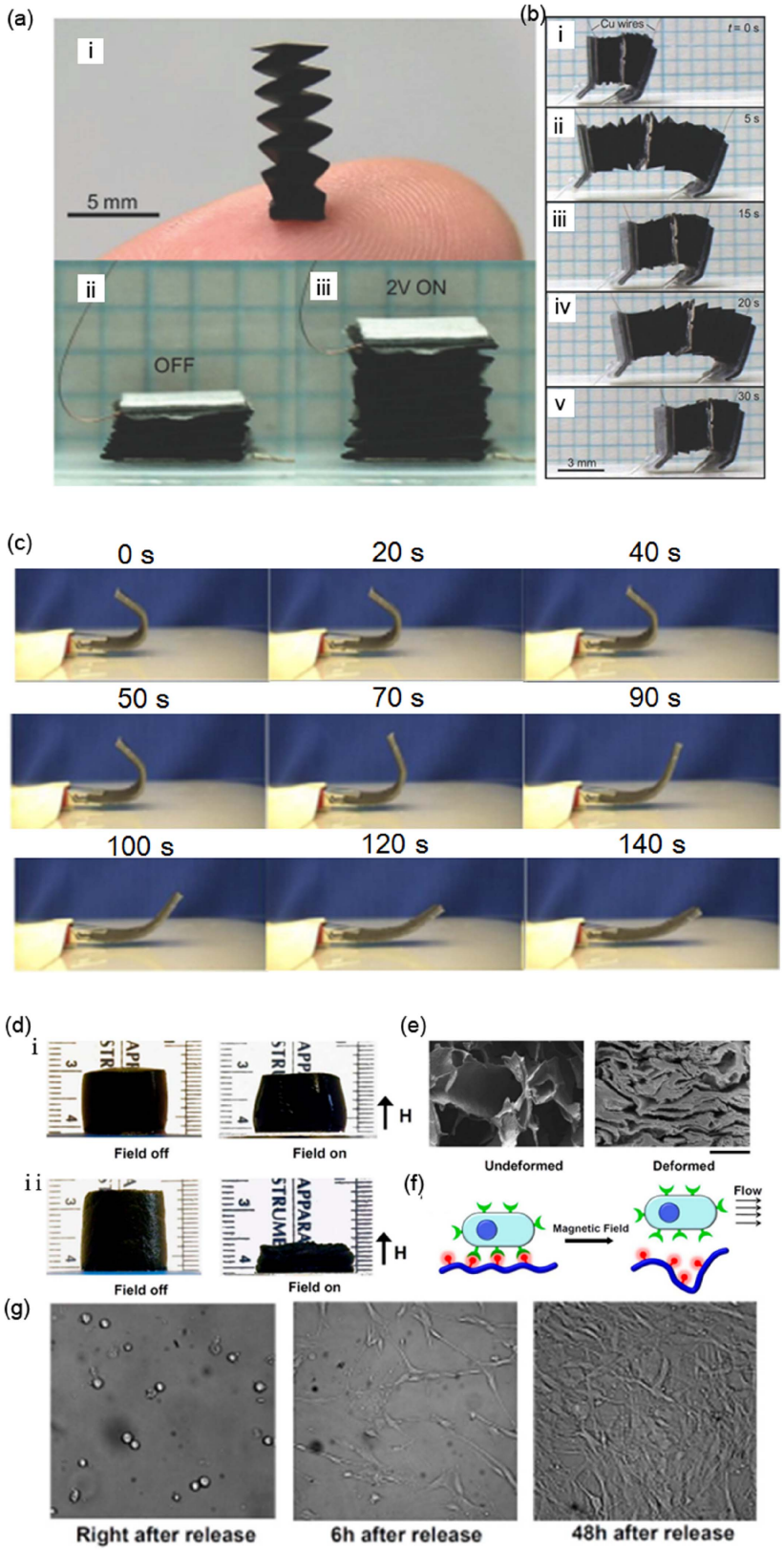

Figure 6. (a) The fabrication process of electrical-responsive construct (a) (i) before and after annealing at (a) (ii) 0 V and (a)-(iii) 2 V. (b) (i)–(v) The serial action images of the biomorphic robot. (Reprinted with permission from [112] Copyright (2013) John Wiley & Sons.) (c) Photographs of the shape-memory effect of shape-memory polymer (SMP) material with 1.8 g carbon nanofiber (CNF) nanopaper. (Reprinted with permission from [115] Copyright (2013) IOP Publishing.) (d) (i) A nanoporous ferrogel decreased its height of 5% under a vertical magnetic field. (d) (ii) The macroporous ferrogel reduced its height of nearly 70% under the same magnetic field. (e) SEM images of a freeze-dried macroporous ferrogel at undeformed/deformed states. Scale bar = 500 μm. (f) Mechanism of marcoporous gel deformation and release of cells carried by outflowing medium. (g) Proliferation and spreading of the released cells from the ferrogels replanted on the culture dish. (Reprinted with permission from [120] Copyright (2010) National Academy of Sciences.)

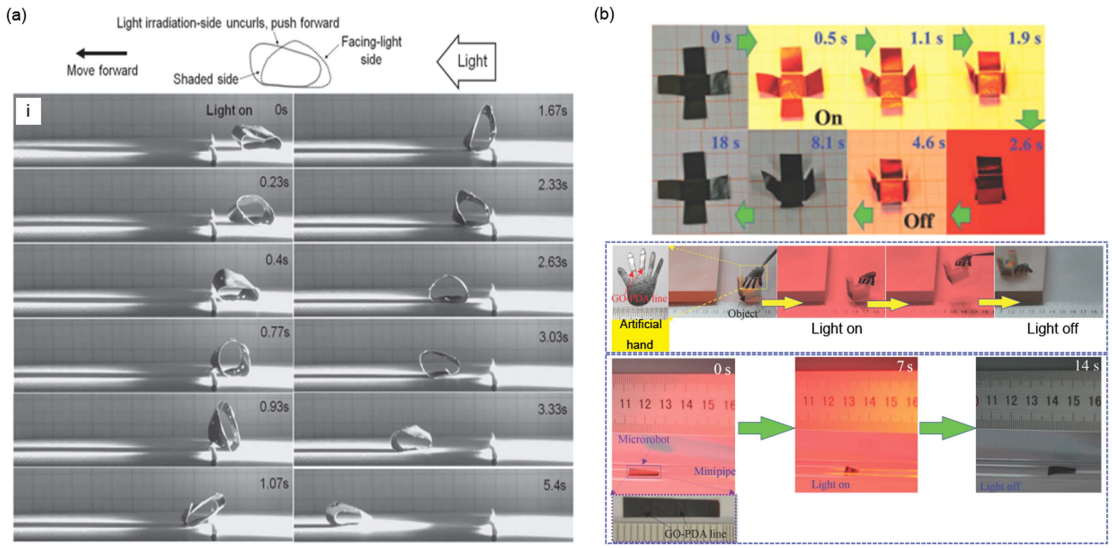

Figure 7. (a) (i) Photographs of the motion of a crawler-type robot fabricated by rGO/CNT-coated PDMS driven by light to pass across an obstacle. (Reprinted with permission from [129] Copyright (2015) John Wiley & Sons.) (b) Transformation of a box and a robotic hand, and the movement of a microrobot, all based on GO-PDA nanopaper triggered by light irradiation. (Reprinted with permission from [130] Copyright (2015) American Association for the Advancement of Science.)

electrical-/magnetic-sensitive materials have the potential to be applied to 4D bioprinting, local changes of pH value and temperature of the medium might occur during the electrical or magnetic stimulations. To prevent the changes that may cause adverse effects on cells, it is necessary to optimize the voltage of the electrical field and intensity of the magnetic field when triggering the transformation of the 4D bioprinting structures.

4.2.4. Light-responsive materials

Light-sensitive materials may convert externally applied optical stimulant into mechanical responses in a more precise manner than the previously mentioned stimuli since light can be conveniently pinpointed to the location of interest [121, 122]. Optical stimuli may be applied to a localized region at extremely high spatial resolution, where the light intensity can directly modulate the behaviors of these materials. Photoisomerization and photodegradation in the polymer chains are the most important mechanisms for light-responsive materials [123–125], which have been widely applied in switches, artificial muscles, and robotics [126]. Recently, CNT and graphene-based materials are considered as good candidates for their usage as light-sensitive elements due to the large aromatic (π-configuration) interface that endows them with excellent optical responsiveness (i.e. photothermal effect) in addition to the electrical properties [114, 127, 128]. Chen and colleagues combined reduced graphene oxide (rGO), CNT, and poly (dimethylsiloxane) (PDMS) to fabricate a crawler-type robot [129]. When one side of this robot was faced with a light source it started to expand due to heating, while the transformation on the shaded side was much smaller due to the lack of irradiation, thus inducting the robot to continuously roll forward (figure 7(a)). This observation revealed that the rGO/CNT-based robot had the capability to rapidly and continuously respond to optical stimulation.

Moreover, Zhu and co-workers presented other applications of light-responsive graphene-based materials [130]. They used a polydopamine-functionalized GO nanosheet (GO-PDA nanosheet) to fabricate a flat pattern. The GO-PDA paper implemented a directed transformation to form a box after 2.6 s upon exposure of a near-infrared (NIR) light, which could reverse back to the original shape after release of the light (figure 7(b)). Based on the same concept, an artificial hand and a microbot were further assembled. As shown in figures 7(c) and (d), the artificial hand could fold, grasp, and even hold an object when stimulated with NIR light, whereas the microbot crawled forward upon the same stimulation. The major advantages of this type of light-triggered transformation lies in its precision and the ability for remote control. Additionally, Tirrell, Anseth, and their colleagues utilized PEG-based hydrogels to create another category of light-responsive materials that possessed photodegradation ability. Tirrell and co-workers synthesized a light-responsive hydrogel based on PEG doped with a photo-labile peptide (N_3–DGPQGIWGQGDK(N_3)–NH_2) through a strain-promoted azide-alkyne cycloaddition reaction [109]. They could regulate the immobilization and release of proteins in desired patterns within the 3D hydrogel by the oxime-ligation and the ortho-nitroenzyl ester photocleavage reactions, respectively, upon exposure of light at selected wavelengths. On the other hand, Anseth and co-workers developed a photodegradable hydrogel by the use of a photodegradable crosslinker, arginine-glycine-aspartic acid-serine (RGDS) tether polymerized with

PEG monomarylate (PEGA) [124]. Under proper light stimulation, 3D features in the hydrogel could be generated due to localized degradation. Cells were also encapsulated in this material where they could be directed to migrate along the degraded patterns [131]. Moreover, they also confirmed that the chondrogenic differentiation of human mesenchymal stem cells and glycosaminoglycans production could be enhanced when the RGDS tether was cleaved. These results indicated that the cells could sense and actively respond to the changes of the dynamic microenvironments.

Light-responsiveness has so far been widely applied in a wide range of biomedical applications such as controlled drug delivery or cancer therapy [132]. To extend its applications to 4D bioprinting, it is envisioned that they can be rationally combined with existing bioinks to allow for direct bioprinting followed by optical stimulation, to achieve desired deformation or degradation of hydrogels and thus fabrication of biological constructs and biomimetic robotics. The strong attenuation of light by biological tissues may post a challenge to this strategy causing non-uniform illumination and transformation. Alternatively, NIR light sources can be used to improve the penetration of light in bioprinted photo-sensitive tissue constructs.

5. Conclusions and perspective

Overall, significant advancements have been achieved in the evolution of 3D printing technologies during the past few decades. In particular, 3D bioprinting that utilizes 3D printers to fabricate objects from biomaterials and cellular species have seen tremendous progress in the last 5–10 years. Merging smart biomaterials with innovative instrumentation, 4D bioprinting is now expected to become the next-generation technology to create transformable objects for applications in biomedicine. Essentially, 4D bioprinting endows patterned structures with the unique ability to transform by exploiting the shape-changing features of the various types of stimuli-responsive biomaterials. The innovative technology has paved new avenues to fabricate sophisticated structures with on-demand dynamically controllable shapes by integrating an additional dimension of time.

However, several challenges remain that need to be addressed to make a great leap to this exciting new field. First and foremost, the bioinks have to be optimized to achieve successful bioprinting. The myriad types of stimuli-responsive biomaterials discussed above, although have been thoroughly investigated for the properties and used to generate constructs via conventional biofabrication approaches, their direct translation for usage as the bioinks may not be straightforward. Ideally a bioink should possess a few basic properties [13, 133, 134]: (i) strong biocompatibility to ensure proper cellular behaviors and functionality for the bioprinted objects; (ii) appropriate rheological parameters to ensure proper printability [11, 135–137]; (iii) suitable stabilization mechanisms, either physical (e.g. ion-induced, thermal) gelation or chemical crosslinking to ensure the architectural integrity of the bioprinted structures [60, 135]; and (iv) the interplay between the cellular viability/function and the dynamic modulation of the bioprinted objects, where it has to be ensured that the cells can survive the stimuli necessary to endow these 4D bioprinted materials with shape-changing capacity while such capacity should not be diminished by the inclusion of cells. Therefore, engineering the properties of existing stimuli-responsive biomaterials has become extremely important to render them compatible with the requirements for use as bioinks, thus achieving 4D bioprinting.

Furthermore, ways to obtain robust shape-changing capability of the 4D bioprinted constructs poses another challenge. For example, Tibbits and colleagues proved that the mechanical properties of printed objects degraded severely after repeatedly execution of folding/unfolding procedures, where the scaffolds could only fully recover to its original shape for a small number of repeated processes [70]. To this end, it is imperative to design the mechanics of the stimuli-responsive bioinks and thus printed constructs especially when repeated responsiveness is desired.

Moreover, complexity in the shape transformation also needs improvement to suit for increasing demand in 4D bioprinting to construct objects of a wide spectrum of applications. For example, biological tissues typically require multiple folding processes to achieve full functionality especially for those undergoing development, and biorobotics may need on-demand, repeated but distinctive folding events to render them desired utilities. To advance the innovation in 4D bioprinting, it is consequently crucial to incorporate rational computer designs of sophisticated multiple stimuli-responsive procedures in order to further boost its dissemination in building complex self-morphing objects for widespread applications in biomedicine such as tissue engineering, soft robotics, and biomedical devices.

References

[1] Khademhosseini A *et al* 2009 Progress in tissue engineering *Sci. Am.* **300** 64–71
[2] Atala A *et al* 2012 Engineering complex tissues *Sci. Transl. Med.* **4** 160rv112
[3] Zhang Y S and Xia Y 2015 Multiple facets for extracellular matrix mimicking in regenerative medicine *Nanomedicine* **10** 689–92
[4] Leijten J *et al* 2015 Advancing tissue engineering: a tale of nano, micro and macro scale integration *Small* **12** 2130–45
[5] Huh D *et al* 2011 From 3D cell culture to organs-on-chips *Trends Cell Biol.* **21** 745–54
[6] Bhise N S *et al* 2014 Organ-on-a-chip platforms for studying drug delivery systems *J. Control. Release* **190** 82–93
[7] Ebrahimkhani M R *et al* 2014 Approaches to *in vitro* tissue regeneration with application for human disease

modeling and drug development *Drug. Discov. Today* **19** 754–62
[8] Moya M L and George S C 2014 Integrating *in vitro* organ-specific function with the microcirculation *Curr. Opin. Chem. Eng.* **3** 102–11
[9] Zhang Y S and Khademhosseini A 2015 Seeking the right context for evaluating nanomedicine: from tissue models in petri dishes to microfluidic organs-on-a-chip *Nanomedicine* **10** 685–8
[10] Jang H L *et al* 2016 Boosting clinical translation of nanomedicine *Nanomedicine* **11** 1495–7
[11] Murphy S V and Atala A 2014 3D bioprinting of tissues and organs *Nat. Biotechnol.* **32** 773–85
[12] Malda J *et al* 2013 25th anniversary article: engineering hydrogels for biofabrication *Adv. Mater.* **25** 5011–28
[13] Zhang Y S *et al* 2016 3D Bioprinting for tissue and organ fabrication *Ann. Biomed. Eng.* (doi:10.1007/s10439-016-1612-8)
[14] Hull C W 1986 Apparatus for production of three-dimensional objects by stereolithographUS Patent US4575330 A
[15] Hutmacher D W *et al* 2001 Mechanical properties and cell cultural response of polycaprolactone scaffolds designed and fabricated via fused deposition modeling *J. Biomed. Mater. Res.* **55** 203–16
[16] Mullen L *et al* 2009 Selective laser melting: a regular unit cell approach for the manufacture of porous, titanium, bone in-growth constructs, suitable for orthopedic applications *J. Biomed. Mater. Res.* B **89** 325–34
[17] Nakamura M *et al* 2010 Biomatrices and biomaterials for future developments of bioprinting and biofabrication *Biofabrication* **2** 014110
[18] Zopf D A *et al* 2013 Bioresorbable airway splint created with a three-dimensional printer *New Engl. J. Med.* **368** 2043–5
[19] Leong K F *et al* 2001 Fabrication of porous polymeric matrix drug delivery devices using the selective laser sintering technique *Proc. Inst. Mech. Eng.* H **215** 191–201
[20] Norotte C *et al* 2009 Scaffold-free vascular tissue engineering using bioprinting *Biomaterials* **30** 5910–7
[21] Xu F *et al* 2011 A three-dimensional *in vitro* ovarian cancer coculture model using a high-throughput cell patterning platform *Biotechnol. J.* **6** 204–12
[22] Zhang Y S *et al* 2016 Bioprinting the cancer microenvironment *ACS Biomater. Sci. Eng.* **2** 1710–21
[23] Lu L *et al* 2013 Design and validation of a bioreactor for simulating the cardiac niche: a system incorporating cyclic stretch, electrical stimulation, and constant perfusion *Tissue Eng.* A **19** 403–14
[24] Zakhem E *et al* 2015 The appendix as a viable source of neural progenitor cells to functionally innervate bioengineered gastrointestinal smooth muscle tissues *Stem Cells Transl. Med.* **4** 548–54
[25] Nagy J I *et al* 2014 Functional alterations in gut contractility after connexin36 ablation and evidence for gap junctions forming electrical synapses between nitrergic enteric neurons *FEBS Lett.* **588** 1480–90
[26] Yalcin S *et al* 2013 Ureterovesical junction obstruction causes increment in smooth muscle contractility, and cholinergic and adrenergic activity in distal ureter of rabbits *J. Pediatr. Surg.* **48** 1954–61
[27] Lee M P *et al* 2015 Development of a 3D printer using scanning projection stereolithography *Sci. Rep.* **5** 9875
[28] Lin D *et al* 2015 3D stereolithography printing of graphene oxide reinforced complex architectures *Nanotechnology* **26** 434003
[29] Tumbleston J R *et al* 2015 Additive manufacturing. Continuous liquid interface production of 3D objects *Science* **347** 1349–52
[30] Chen H *et al* 2016 Application of FDM three-dimensional printing technology in the digital manufacture of custom edentulous mandible trays *Sci. Rep.* **6** 19207
[31] Bernhard Mueller D K 1999 Laminated object manufacturing for rapid tooling and patternmaking in foundry industry *Comput. Ind.* **39** 47–53
[32] Stamp R *et al* 2009 The development of a scanning strategy for the manufacture of porous biomaterials by selective laser melting *J. Mater. Sci., Mater. Med.* **20** 1839–48
[33] Williams J M *et al* 2005 Bone tissue engineering using polycaprolactone scaffolds fabricated via selective laser sintering *Biomaterials* **26** 4817–27
[34] Das S 2003 Physical aspects of process control in selective laser sintering of metals *Adv. Eng. Mater.* **5** 701–11
[35] Sheth R *et al* 2016 Three-dimensional printing: an enabling technology for IR *J. Vasc. Interv. Radiol.* **27** 859–65
[36] Ma X *et al* 2016 Deterministically patterned biomimetic human iPSC-derived hepatic model via rapid 3D bioprinting *Proc. Natl Acad. Sci. USA* **113** 2206–11
[37] Zhu W *et al* 2016 3D printing of functional biomaterials for tissue engineering *Curr. Opin. Biotechnol.* **40** 103–12
[38] Gou M *et al* 2014 Bio-inspired detoxification using 3D-printed hydrogel nanocomposites *Nat. Commun.* **5** 3774
[39] Zhu W *et al* 2015 3D-printed artificial microfish *Adv. Mater.* **30** 4411–7
[40] Tekin E *et al* 2008 Inkjet printing as a deposition and patterning tool for polymers and inorganic particles *Soft Matter* **4** 703–13
[41] Fang Y *et al* 2012 Rapid generation of multiplexed cell cocultures using acoustic droplet ejection followed by aqueous two-phase exclusion patterning *Tissue Eng.* C **18** 647–57
[42] Cohen D L *et al* 2006 Direct freeform fabrication of seeded hydrogels in arbitrary geometries *Tissue Eng.* **12** 1325–35
[43] Khalil S and Sun W 2007 Biopolymer deposition for freeform fabrication of hydrogel tissue constructs *Mater. Sci. Eng.* C **27** 469–78
[44] Chrisey D B 2000 Materials processing: the power of direct writing *Science* **289** 879–81
[45] Colina M *et al* 2005 DNA deposition through laser induced forward transfer *Biosens. Bioelectron.* **20** 1638–42
[46] Ringeisen B R *et al* 2004 Laser printing of pluripotent embryonal carcinoma cells *Tissue Eng.* **10** 483–91
[47] Zhang Z *et al* 2016 Study of impingement types and printing quality during laser printing of viscoelastic alginate solutions *Langmuir* **32** 3004–14
[48] Xu C *et al* 2014 Study of droplet formation process during drop-on-demand inkjetting of living cell-laden bioink *Langmuir* **30** 9130–8
[49] Xiong R *et al* 2015 Freeform drop-on-demand laser printing of 3D alginate and cellular constructs *Biofabrication* **7** 045011
[50] Jakus A E *et al* 2016 Advancing the field of 3D biomaterial printing *Biomed. Mater.* **11** 014102
[51] Blaeser A *et al* 2016 Controlling shear stress in 3D bioprinting is a key factor to balance printing resolution and stem cell integrity *Adv. Healthcare Mater.* **5** 326–33
[52] Colosi C *et al* 2015 Microfluidic bioprinting of heterogeneous 3D tissue constructs using low viscosity bioink *Adv. Mater.* **28** 677–84
[53] Bhattacharjee T *et al* 2015 Writing in the granular gel medium *Sci. Adv.* **1** e1500655
[54] Highley C B *et al* 2015 Direct 3D printing of shear-thinning hydrogels into self-healing hydrogels *Adv. Mater.* **27** 5075–9
[55] Hinton T J *et al* 2015 Three-dimensional printing of complex biological structures by freeform reversible embedding of suspended hydrogels *Sci. Adv.* **1** e1500758
[56] Chang R *et al* 2008 Effects of dispensing pressure and nozzle diameter on cell survival from solid freeform fabrication-based direct cell writing *Tissue Eng.* A **14** 41–8
[57] Campbell J *et al* 2015 Multimaterial and multiscale three-dimensional bioprinter *J. Nanotechnol. Eng. Med.* **6** 021005
[58] Ober T J *et al* 2015 Active mixing of complex fluids at the microscale *Proc. Natl Acad. Sci. USA* **112** 12293–8
[59] Kang H-W *et al* 2016 A 3D bioprinting system to produce human-scale tissue constructs with structural integrity *Nat. Biotechnol.* **34** 312–9
[60] Kolesky D B *et al* 2014 3D bioprinting of vascularized, heterogeneous cell-laden tissue constructs *Adv. Mater.* **26** 3124–30

[61] Hardin J O *et al* 2015 Microfluidic printheads for multimaterial 3D printing of viscoelastic inks *Adv. Mater.* **27** 3279–84
[62] Asthana A and Kisaalita W S 2015 Is time an extra dimension in 3D cell culture? *Drug Discovery Today* **21** 305–99
[63] Burdick J A and Murphy W L 2012 Moving from static to dynamic complexity in hydrogel design *Nat. Commun.* **3** 1269
[64] Lang R J 2011 *Origami Design Secrets: Mathematical Methods for an Ancient Art* (Natick, MA: AK Peters, Ltd)
[65] Li Q and Lewis J A 2003 Nanoparticle inks for directed assembly of three-dimensional periodic structures *Adv. Mater.* **15** 1639–43
[66] Montroll J and Lang R J 2003 *Origami Sea Life* (New York: Dover)
[67] Ahn B Y *et al* 2010 Printed origami structures *Adv. Mater.* **22** 2251–4
[68] Anfinsen C B 1973 Principles that govern the folding of protein chains *Science* **181** 223–30
[69] Mahadevan L and Rica S 2005 Self-organized origami *Science* **307** 1740
[70] Raviv D *et al* 2014 Active printed materials for complex self-evolving deformations *Sci. Rep.* **4** 7422
[71] Sydney Gladman A *et al* 2016 Biomimetic 4D printing *Nat. Mater.* **15** 413–8
[72] Compton B G and Lewis J A 2014 3D-printing of lightweight cellular composites *Adv. Mater.* **26** 5930–5
[73] Smay J E *et al* 2002 Colloidal inks for directed assembly of 3D periodic structures *Langmuir* **18** 5429–37
[74] Kokkinis D *et al* 2015 Multimaterial magnetically assisted 3D printing of composite materials *Nat. Commun.* **6** 8643
[75] Tan J L *et al* 2003 Cells lying on a bed of microneedles: an approach to isolate mechanical force *Proc. Natl Acad. Sci. USA* **100** 1484–9
[76] Maruthamuthu V *et al* 2011 Cell-ECM traction force modulates endogenous tension at cell–cell contacts *Proc. Natl Acad. Sci. USA* **108** 4708–13
[77] Brugués A *et al* 2014 Forces driving epithelial wound healing *Nat. Phys.* **10** 683–90
[78] Underwood C J *et al* 2014 Cell-generated traction forces and the resulting matrix deformation modulate microvascular alignment and growth during angiogenesis *Am. J. Physiol. Heart. Circ. Physiol.* **307** H152–64
[79] Kraning-Rush C M *et al* 2012 Cellular traction stresses increase with increasing metastatic potential *PLoS One* **7** e32572
[80] Tranquillo R T and Murray J D 1992 Continuum model of fibroblast-driven wound contraction: inflammation-mediation *J. Theor. Biol.* **158** 135–72
[81] Franze K 2013 The mechanical control of nervous system development *Development* **140** 3069–77
[82] Lakirev A V and Belousov L V 1986 Computer modelling of gastrulation and neurulation in amphibian embryos based on mechanical tension fields *Ontogenez* **17** 636–47
[83] Kuribayashi-Shigetomi K *et al* 2012 Cell origami: self-folding of three-dimensional cell-laden microstructures driven by cell traction force *PLoS One* **7** e51085
[84] Fratzl P and Barth F G 2009 Biomaterial systems for mechanosensing and actuation *Nature* **462** 442–8
[85] Skotheim J M and Mahadevan L 2005 Physical limits and design principles for plant and fungal movements *Science* **308** 1308–10
[86] Elbaum R *et al* 2007 The role of wheat awns in the seed dispersal unit *Science* **316** 884–6
[87] Huang X *et al* 2015 Palladium-catalyzed triple cyclization of 2, 7-alkadiynylic carbonates with allenes bearing a carbon nucleophile *Chemistry* **21** 15540–3
[88] Dai M *et al* 2013 Humidity-responsive bilayer actuators based on a liquid-crystalline polymer network *ACS Appl. Mater. Interfaces* **5** 4945–50
[89] Zhang L *et al* 2015 Photogated humidity-driven motility *Nat. Commun.* **6** 7429
[90] Zhang K *et al* 2015 Moisture-responsive films of cellulose stearoyl esters showing reversible shape transitions *Sci. Rep.* **5** 11011
[91] Klouda L and Mikos A G 2008 Thermoresponsive hydrogels in biomedical applications *Eur. J. Pharm. Biopharm.* **68** 34–45
[92] Peppas N A *et al* 2000 Hydrogels in pharmaceutical formulations *Eur. J. Pharm. Biopharm.* **50** 27–46
[93] Li L *et al* 2002 Thermally induced association and dissociation of methylcellulose in aqueous solutions *Langmuir* **18** 7291–8
[94] Ron E S and Bromberg L E 1998 Temperature-responsive gels and thermogelling polymer matrices for protein and peptide delivery *Adv. Drug. Deliv. Rev.* **31** 197–221
[95] Ayano E and Kanazawa H 2014 Temperature-responsive smart packing materials utilizing multi-functional polymers *Anal. Sci.* **30** 167–73
[96] Chen Q *et al* 2015 Fundamentals of double network hydrogels *J. Mater. Chem.* B **3** 3654–76
[97] Haque M A, Kurokawa T and Gong J P 2012 Super tough double network hydrogels and their application as biomaterials *Polymer* **53** 1805–22
[98] Li G *et al* 2015 Poly(vinyl alcohol)-poly(ethylene glycol) double-network hydrogel: a general approach to shape memory and self-healing functionalities *Langmuir* **31** 11709–16
[99] Ricciardi R *et al* 2004 X-ray diffraction analysis of poly(vinyl alcohol) hydrogels, obtained by freezing and thawing techniques *Macromolecules* **37** 1921–7
[100] Wang D *et al* 2015 Intelligent rubber with tailored properties for self-healing and shape memory *J. Mater. Chem.* A **3** 12864–72
[101] Okano T *et al* 1993 A novel recovery system for cultured cells using plasma-treated polystyrene dishes grafted with poly(N-isopropylacrylamide) *J. Biomed. Mater. Res.* **27** 1243–51
[102] Pei Y *et al* 2004 The effect of pH on the LCST of poly(N-isopropylacrylamide) and poly(N-isopropylacrylamide-co-acrylic acid) *J. Biomater. Sci. Polym. Ed.* **15** 585–94
[103] Breger J C *et al* 2015 Self-folding thermo-magnetically responsive soft microgrippers *ACS Appl. Mater. Interfaces* **7** 3398–405
[104] Luo R *et al* 2015 Gradient porous elastic hydrogels with shape-memory property and anisotropic responses for programmable locomotion *Adv. Funct. Mater.* **25** 7272–9
[105] Bakarich S E *et al* 2015 4D printing with mechanically robust, thermally actuating hydrogels *Macromol. Rapid Commun.* **36** 1211–7
[106] Borisova O V *et al* 2015 pH- and electro-responsive properties of poly(acrylic acid) and poly(acrylic acid)-block-poly(acrylic acid-grad-styrene) brushes studied by quartz crystal microbalance with dissipation monitoring *Langmuir* **31** 7684–94
[107] Neveln I D *et al* 2013 Biomimetic and bio-inspired robotics in electric fish research *J. Exp. Biol.* **216** 2501–14
[108] Shi H *et al* 2015 A review: fabrications, detections and applications of peptide nucleic acids (PNAs) microarray *Biosens. Bioelectron.* **66** 481–9
[109] Song E and Choi J-W 2013 Conducting polyaniline nanowire and Its applications in chemiresistive sensing *Nanomaterials* **3** 488–523
[110] Wong J Y *et al* 1994 Electrically conducting polymers can noninvasively control the shape and growth of mammalian cells *Proc. Natl Acad. Sci. USA* **91** 3201–4
[111] Okuzaki H *et al* 2008 A biomorphic origami actuator fabricated by folding a conducting paper *J. Phys.: Conf. Ser.* **012001**
[112] Okuzaki H *et al* 2013 Humidity-sensitive polypyrrole films for electro-active polymer actuators *Adv. Funct. Mater.* **23** 4400–7
[113] Bandaru P R 2007 Electrical properties and applications of carbon nanotube structures *J. Nanosci. Nanotechnol.* **7** 1239–67
[114] Shin S R *et al* 2016 Graphene-based materials for tissue engineering *Adv. Drug. Deliv. Rev.* **105** 255–74

[115] Lu H *et al* 2010 Electrical properties and shape-memory behavior of self-assembled carbon nanofiber nanopaper incorporated with shape-memory polymer *Smart Mater. Struct.* **19** 075021
[116] Lu A H *et al* 2007 Magnetic nanoparticles: synthesis, protection, functionalization, and application *Angew. Chem., Int. Ed. Engl.* **46** 1222–44
[117] Gupta A K and Gupta M 2005 Synthesis and surface engineering of iron oxide nanoparticles for biomedical applications *Biomaterials* **26** 3995–4021
[118] Hu S H *et al* 2008 Core/single-crystal-shell nanospheres for controlled drug release via a magnetically triggered rupturing mechanism *Adv. Mater.* **20** 2690–5
[119] Hu S H *et al* 2007 Nano-ferrosponges for controlled drug release *J. Control. Release* **121** 181–9
[120] Zhao X *et al* 2011 Active scaffolds for on-demand drug and cell delivery *Proc. Natl Acad. Sci. USA* **108** 67–72
[121] Lima M D *et al* 2012 Electrically, chemically, and photonically powered torsional and tensile actuation of hybrid carbon nanotube yarn muscles *Science* **338** 928–32
[122] Koerner H *et al* 2004 Remotely actuated polymer nanocomposites—stress-recovery of carbon-nanotube-filled thermoplastic elastomers *Nat. Mater.* **3** 115–20
[123] Irie M 1990 *New Polymer Materials* (Berlin: Springer) pp 27–67
[124] Kloxin A M *et al* 2009 Photodegradable hydrogels for dynamic tuning of physical and chemical properties *Science* **324** 59–63
[125] DeForest C A and Tirrell D A 2015 A photoreversible protein-patterning approach for guiding stem cell fate in three-dimensional gels *Nat. Mater.* **14** 523–31
[126] Raman R *et al* 2016 Optogenetic skeletal muscle-powered adaptive biological machines *Proc. Natl Acad. Sci. USA* **113** 3497–502
[127] Park S *et al* 2010 Graphene-based actuators *Small* **6** 210–2
[128] Li C *et al* 2011 Reversible white-light actuation of carbon nanotube incorporated liquid crystalline elastomer nanocomposites *Soft Matter* **7** 7511–6
[129] Hu Y *et al* 2015 A graphene-based bimorph structure for design of high performance photoactuators *Adv. Mater.* **27** 7867–73
[130] Mu J *et al* 2015 Origami-inspired active graphene-based paper for programmable instant self-folding walking devices *Sci. Adv.* **1** e1500533
[131] Nicodemus G D and Bryant S J 2008 Cell encapsulation in biodegradable hydrogels for tissue engineering applications *Tissue Eng.* B **14** 149–65
[132] Qin Y *et al* 2015 Near-infrared light remote-controlled intracellular anti-cancer drug delivery using thermo/pH sensitive nanovehicle *Acta Biomater.* **17** 201–9
[133] Chimene D *et al* 2016 Advanced bioinks for 3D printing: a materials science perspective *Ann. Biomed. Eng.* **44** 1–13
[134] Jungst T *et al* 2015 Strategies and molecular design criteria for 3D printable hydrogels *Chem. Rev.* **116** 1496–539
[135] Chung J H Y *et al* 2013 Bio-ink properties and printability for extrusion printing living cells *Biomater. Sci.* **1** 763–73
[136] Murphy S V *et al* 2013 Evaluation of hydrogels for bio-printing applications *J. Biomed. Mater. Res.* A **101** 272–84
[137] Skardal A and Atala A 2015 Biomaterials for integration with 3D bioprinting *Ann. Biomed. Eng.* **43** 730–46